

## COBEM-2017-1859

# A STUDY OF ATTITUDE AND HEADING DETERMINATION THROUGH AN EKF-BASED SENSOR FUSION FOR INERTIAL MEASUREMENT UNITS (IMUs)

Fabián Barrera Prieto

Renato C. Sampaio

Daniel M. Muñoz

Carlos H. Llanos

Universidade de Brasília, Department of Mechanical Engineering, Brasília, Brazil  
fbarrera6@gmail.com, llanos@unb.br, renatocoral@unb.br, damuz23@gmail.com

**Abstract.** This paper presents the study and design of a sensor fusion technique for Inertial Measurement Units (IMUs) of 6 and 9 degrees of freedom (DOF), in order to determine the attitude (roll and pitch) and heading (yaw) using the Extended Kalman Filter (EKF). The IMUs chosen are the MPU6050 (6 DOF, comprising accelerometer and gyroscope) and the MPU9250 (9 DOF, comprising accelerometer, gyroscope and magnetometer). In order to estimate both the attitude and heading of each IMU a sensor fusion technique based on the use of a gyroscope as the system model and both the accelerometer and the magnetometer as measurement models were used. For the sensor fusion design the EKF has been chosen due to the fact that the system model is highly non-linear. The calibration and tests of the IMUs was performed in a platform, manufactured in a 3D printer. Additionally, simulation results show that the technique used for the sensor fusion presents good quality for both attitude and heading estimation for the two IMUs.

**Keywords:** Sensor Fusion, Extend Kalman Filter, Inertial Measurement Units, MPU6050, MPU9250, Attitude, Heading.

## 1. INTRODUCTION

The IMUs are Microelectromechanical Systems (MEMS) developed for a wide range of applications such as robotics, computational vision and artificial intelligence, among others. The main components of these inertial units are: (a) a power supply (3.3V), (b) a processor, (c) sensors and (d) a communication interface (I2C, SPI). Commonly, the sensors that compose the IMU are the accelerometer, the gyroscope and the magnetometer, providing gravitational forces, speed and rotation measurements. Nowadays, it is also common to find IMUs with barometer, altimeter, temperature sensors, among others (Ahmad *et al.*, 2013). Each embedded sensor in an IMU can measure in the three reference axes (namely,  $X$ ,  $Y$  and  $Z$ ). Sensor fusion techniques aim to combine the information provided by two or more sensors, in order to obtain a better estimative of the state variable(s) with the best possible quality, thus reducing the uncertainty of the estimation. In the case of IMUs, the sensor fusion consists of combining the information of the gyroscope with the accelerometer and magnetometer, allowing the variable of interest (such as inclination, orientation, shock, vibration, among others) to be estimated close to the real value.

The Extended Kalman Filter (EKF) is one of the nonlinear versions of the Kalman Filter, which linearises the state vector through the current mean and covariance. This estimator has been widely regarded in navigation systems (Li and Xu, 2010), through the representation of Euler angles, which are coordinates (*roll*, *pitch* and *yaw*) that serve to specify the orientation and position of a mobile system, with respect to another fixed system. The EKF can be configured for sensor fusion by using information from the gyroscope as the system model, and both data from the accelerometer and magnetometer as the measurement models. This work presents an approach for attitude and heading determination using two EKFs modules for the IMUs, MPU6050 and MPU9250. In the first module (EKF1) the gyroscope and accelerometer data are used to estimate attitude (*roll* and *pitch*). In the second module (EKF2), the heading (*yaw*) is estimated from the fusion between the gyroscope and the magnetometer.

One of the main contributions of this work is the development of a calibration and test platform of IMUs, as well as presenting good attitude and heading estimation results for low cost IMUs, commonly used in commercial and industrial applications; in addition to facilitating the understanding of important topics such as sensors calibration and sensor fusion.

## 2. ATTITUDE AND HEADING WITH EKF

Both the attitude and the heading is the reference system used in navigation applications, which specifies the movements of an object or body (rotation and orientation) in the horizontal plane as well as in the vertical plane, through the Euler angles (*roll*, *pitch* and *yaw*). *Roll* is the angle corresponding to the *X* axis, *pitch* on the *Y* axis and *yaw* on the *Z* axis. Figure 1 depicts the representation of the Euler angles in a navigation system.

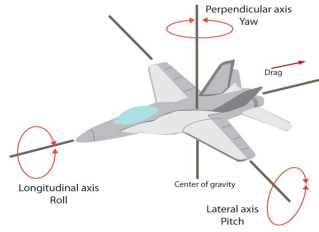


Figure 1. Representation of Euler angles

To estimate these three angles with high precision, MEMS sensors are widely used associated with sensor fusion techniques. This type of sensor has several advantages such as: (a) low cost, (b) high sensitivity, (c) compact (single silicon chip), (d) practical (size), and (e) low power consumption. The size of MEMS ranges from  $1\mu\text{m}$  to  $1\text{mm}$ .

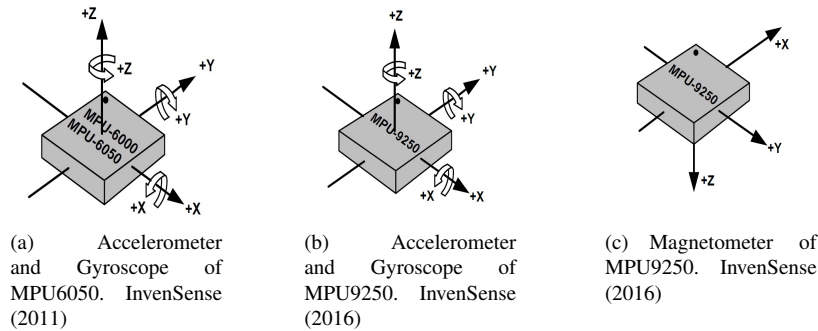


Figure 2. Orthogonal axes and reference angles of IMUs.

Figure 2 shows the respective orthogonal axes and reference angles of IMUs utilized in this work, the MPU6050 and MPU9250 with 6 and 9 degrees of freedom (DOF), respectively; both manufactured by InvenSense. In Table 1 the main features of these two devices are presented. It can be observed that the main difference between both IMUs is the implementation of the magnetometer in the case of the IMU of 9DOF.

Table 1. Main features of MPU6050 and MPU9250

FEATURES	MPU6050	MPU9250
Sensors	Gyroscope, Accelerometer	Gyroscope, Accelerometer, Magnetometer
Power supply	2.375V-3.46V	2.4V-3.6V
Package size	16 x 20 mm	15 x 25 mm
Degrees of freedom	6	9
Communication interface	I2C	I2C
Normal operating current*	3.9mA	3.5mA
Operation frequency	400kHz	400kHz
Price	\$5.00	\$18.00
Others	**DMP (Digital Motion Processor) Temperature sensor (-40 to +85°C)	**DMP (Digital Motion Processor) Temperature sensor (-40 to +85°C)

(\*) Operating current when all sensors and the DMP are enabled

(\*\*) DMP is the internal processor of each IMU

### 2.1 Previous works

Several previous works regarding sensor fusion of IMUs based on the EKF estimator were found in the scientific literature. Motion measurement (orientation and position) using a method to compensate the drift error of the inertial sensors (IMU) with the assist of ultrasonic sensors for sensor fusion using EKF. The position measured by the ultrasonic sensor and the orientation measured by the digital compass (magnetometer combined with accelerometer) are defined as

the observation values, and the position, velocity, and orientation are included in the state vector (Zhao and Wang, 2012). A camera pose estimation based on sensor fusion with monocular vision system and IMUs was proposed by (Ligorio and Sabatini, 2013). In this work, the authors developed two EKF filters, each with different methodology, an EKF using a variant of the Direct Linear Transformation (DLT) method, and the other EKF using the projection errors. Indoor localization of a mini-Unmanned Aerial Vehicle (UAV) with IMUs and vision sensors, in which a EKF like technique to improve the localization was used. The proposed approach allows the designer to use a low-cost Inertial Measurement Unit (IMU) in the prediction step, and the integration of vision odometry for the detection of markers nearness the touchdown area (Benini *et al.*, 2013).

## 2.2 Gyroscope

This sensor measures the rotational variations ( $^{\circ}/\text{sec}$ ) exerted on it. MEMS based gyroscopes operate as a result of the Coriolis effect, which consists of generating an external force through a rotating movement on a circular surface. Furthermore, measurements can be made on 1, 2 or 3 orthogonal axes.

The gyroscope measures the angular velocity which is integrated with respect to time, determining the angular position of a body or object. This integration process generates a significant cumulative error in the output signal, being increasing at each iteration; therefore, the measurements of the sensor in a certain time may be far from the correct value. This is the main disadvantage of the gyroscope, also known as *error drift*. The solution to this problem is to filter the output signal. In contrast, the advantage of this sensor is the high precision in the measurements, since the presence of noise in its measurements is almost null. Table 2 presents the features of the gyroscope that is integrated in the MPU6050 and MPU9250. It can be observed that the gyroscope is the same in both IMUs.

Table 2. Features of Gyroscope of the MPU6050 and MPU9250

FEATURES	MPU6050	MPU9250
Measuring axis	Triple-axis (X, Y and Z)	Triple-axis (X, Y and Z)
Dynamic range	$\pm 250, \pm 500, \pm 1000$ and $\pm 2000$ $^{\circ}/\text{seg.}$	$\pm 250, \pm 500, \pm 1000$ and $\pm 2000$ $^{\circ}/\text{seg.}$
Sensitivity Scale Factor	131, 65.6, 32.8, 16.4 LSB/ $(^{\circ}/\text{s})$	131, 65.6, 32.8, 16.4 LSB/ $(^{\circ}/\text{s})$
Output	Digital (16 bits ADCs)	Digital (16 bits ADCs)
Normal operating current	3.6mA	3.2mA

Some of the main applications and use cases of the MEMS gyroscope are: (a) navigation systems, (b) remote control, (c) biomedicine, (d) mobile phones and smart devices, (e) video game consoles, (f) automotive, among others. Figure 3 shows the classification of these applications in relation to the working bandwidth and the dynamic range of the angular velocity (Kraft, 2000).

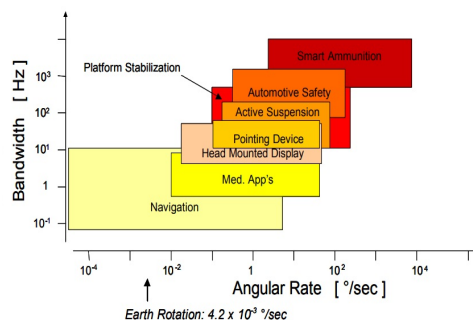


Figure 3. Gyroscope applications according on bandwidth and dynamic angular rate range. (Kraft, 2000)

In the Equations (1), (2) and (3) (Sacco, 2011), the mathematical models to determine the angular position and orientation (Euler angles), using the gyroscope measurements are presented.

$$\dot{\phi} = w_x + w_y \sin \phi \tan \theta + w_z \cos \phi \tan \theta \quad (1)$$

$$\dot{\theta} = w_y \cos \phi - w_z \sin \phi \quad (2)$$

$$\dot{\psi} = w_y \cos \phi \quad (3)$$

## 2.3 Accelerometer

The accelerometer sensor detects the variation of linear velocity that is exerted on it, thus determining the acceleration (in units "g", where 1g is equivalent to  $9.8 \text{ m/s}^2$ ) of the body. The MEMS technology involving accelerometers has

the ability to perform acceleration measurements on 1, 2 or 3 axes; and can be manufactured based on the piezoelectric, piezoresistive and capacitive physical principles. The main advantage of the accelerometer is that the measurements do not have a significant error. Although its major disadvantage is the presence of noise in the measurements so that the output signal of this sensor must be filtered.

The measurements provided by the sensor can be used to estimate different movements of a body or object, such as: (a) acceleration (b) vibration, (b) shock, (c) inclination and (d) rotation. These movements are generated by accelerations in different periods of time (Sacco, 2011). Figure 4 shows the main applications of the accelerometers with respect to the working bandwidth and the dynamic acceleration ranges (Kraft, 2000). Furthermore, from this figure it can be said that an accelerometer with a lower measurement range has a higher sensitivity.

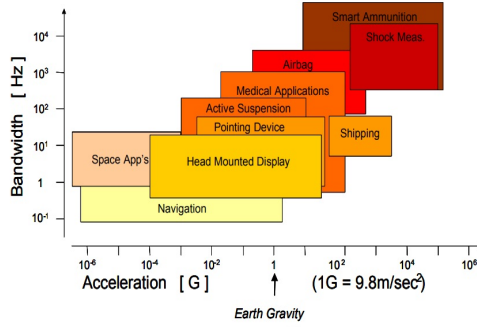


Figure 4. Accelerometer applications according on bandwidth and dynamic acceleration range. (Kraft, 2000)

The features of the accelerometer that is integrated with the MPU6050 and MPU9250 are described in Table 3. In this case, the accelerometer is the same in both the MPU6050 and MPU9250.

Table 3. Features of Accelerometer of the MPU6050 and MPU9250

FEATURES	MPU6050	MPU9250
Measuring axis	Triple-axis (X, Y and Z)	Triple-axis (X, Y and Z)
Dynamic range	±2g, ±4g, ±8g and ±16g	±2g, ±4g, ±8g and ±16g
Sensitivity Scale Factor	16.384, 8.192, 4.096, 2.048 LSB/g	16.384, 8.192, 4.096, 2.048 LSB/g
Output	Digital (16 bits ADCs)	Digital (16 bits ADCs)
Normal operating current	500µA	450µA

Taking into account equations (4) and (5), and the corresponding accelerometer measurements on the three axes ( $a_x$ ,  $a_y$  y  $a_z$ ), two Euler angles can be estimated, specifically *roll* and *pitch* (Ozyagcilar, 2015). The model of accelerometer in the Equation (5) is usually used in applications related to space navigation. Since the *pitch* angle is restricted to  $-90^\circ$  and  $+90^\circ$  its calculation is achieved with the *atan* function. Otherwise, Equation (4) have solutions in the range  $-180^\circ$  and  $+180^\circ$ ; therefore, the *atan2* function can be used in a software application.

$$\phi = \arctan \left( \frac{a_y}{a_z} \right) \tag{4}$$

$$\theta = \arctan \left( \frac{-a_x}{\sqrt{a_y^2 + a_z^2}} \right) \tag{5}$$

## 2.4 Magnetometer

This sensor measures the magnitude of the magnetic field in a given direction and its units of measurement are Teslas “T” or Gauss “G”. The MEMS magnetometer is an electronic device that has the ability to measure up to 3 orthogonal axes (X, Y and Z). Its main application is to estimate the orientation of a body or object through sensor fusion techniques with the gyroscope, being its function equal to that of an electronic compass. This application approach is widely used in navigation systems. Table 4 shows the main features of the magnetometers MPU9250 device. In this case, the magnetometer is just implemented in the MPU9250.

The Equations (6), (7) and (8) present the mathematical models corresponding to the calculation of the third Euler angle (*yaw*) (Ozyagcilar, 2015). Equations (6) and (7) are the components in the axes X and Y of the magnetic field. Equation (8) is restricted only in a range of solutions between  $-180^\circ$  and  $+180^\circ$ ; therefore, it is suitable to use the *atan2* function for this calculation.

$$B_{fy} = m_z \sin \phi - m_y \cos \phi \tag{6}$$

Table 4. Features of Compass of the MPU6050 and MPU9250

FEATURES	MPU6050	MPU9250
Measuring axis	N/A	Triple-axis (X, Y and Z)
Dynamic range	N/A	$\pm 4800\mu\text{T}$
Sensitivity Scale Factor	N/A	1.46 mG/LSB
Output	N/A	Digital (16 bits ADCs)
Normal operating current	N/A	280 $\mu\text{A}$

$$B_{fx} = m_x \cos \theta + m_y \sin \theta \sin \phi + m_z \sin \theta \cos \phi \quad (7)$$

$$\psi = \arctan \left( \frac{-B_{fy}}{B_{fx}} \right) \quad (8)$$

Similar to the MEMS accelerometer the MEMS magnetometer is essential to correct the *drift error* of the Gyroscope for sensor fusion procedure. The main disadvantage of this sensor is that the output signal is unreliable since the measurements have values with little precision (high level of uncertainty) with respect to the real value due to the disturbances of external magnetic fields (for instance from electrical and electronic devices). For which it is necessary to perform a calibration of this sensor before using them in later processes, with the aim of eliminating those perturbations. This drawback (uncalibrated by default) is generated since the manufacturers save manufacturing costs in the sensor calibration. Then, they predict that each user must calibrate the magnetometer to expect good measurement results.

The MEMS magnetometer calibration must be done for each axis. This type of calibration is divided into two parts, called: (a) hard iron and (b) soft iron. The hard iron refers to determine the offset value or bias of the magnetometer, while the soft iron consists of scaling the results of the previous calibration (hard iron). Thus, the soft iron part allows the quality of the magnetometer data to be improved (Winer, 2015).

## 2.5 Sensor fusion technique

Sensor fusion is a process that consists of combining information (measurements) from different sources (sensors), through a fusion mechanism (e.g., a filter estimator), with the main objective of obtaining an output signal with better quality than that could be obtained from a single sensor (NXP, 2016). In Figure 5 the sensor fusion structure is observed through a fusion structure, which can be based on: (a) Kalman filter (KF, EKF or UKF), (b) complementary filter, (c) particle filter, among others. The parameters of the filters must be adjusted in order to improve the sensor fusion results.

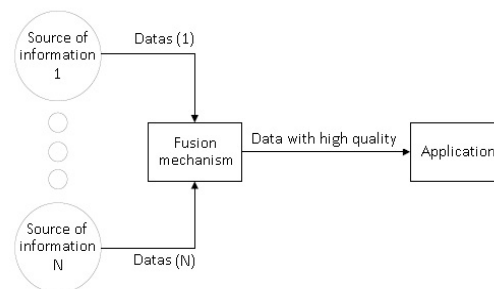


Figure 5. Structure of sensor fusion

This sensor combination technique requires that the available sensors to be complementary to each other, so that the disadvantages of each of the sensors are outweighed by the advantages of the others. Sensor fusion with IMUs is commonly used to find the suitable combination between the gyroscope and the accelerometer (also between the gyroscope and magnetometer) for applications related to navigation systems (for instance, attitude and heading).

## 2.6 Extended Kalman Filter

The Extended Kalman Filter (EKF) is one of the best known stochastic filters in the area of filtering and state estimation for nonlinear systems. The EKF is an algorithm derived from the basic Kalman filter, which is based on linearising the nonlinear system and performing the estimation of the state variables on such linearised system (Kim, 2011). Linearisation is reflected in a Jacobian matrix (A) of partial derivatives of the function  $f(x)$  with regard to each state variable.

Algorithm 1 presents the pseudo-code of the EKF, where it can be observed the 5 main steps of the Kalman filter: (1) predict the state with initial values, (2) compute the error covariance, (3) compute the Kalman gain, (4) update the state estimate and (5) update the error covariance. After step (5) the algorithm returns to step (1) with updated measurements, until a certain number of time steps (N) are reached.

---

**Algorithm 1** Extended Kalman Filter

---

**Require:** Initial values:  $x_0, P_0$ . Measurements:  $z_k$ .

**Ensure:** Estimate and error covariance:  $x_k, P_k$ .

- 1: **for**  $k = 1 : N$  **do**
  - 2:      $x_k^- = f(x_{k-1})$
  - 3:      $P_k^- = AP_{k-1}A^T + Q$
  - 4:      $K_k = P_k^- H^T (HP_k^- H^T + R)^{-1}$
  - 5:      $x_k^+ = x_k^- + K_k(z_k - h(x_k^-))$
  - 6:      $P_k^+ = P_k^- - K_k H P_k^-$
  - 7: **end for**
- 

Where,  $f(x_{k-1})$  and  $h(x_k^-)$  are the predict *state* and *measurements* functions, respectively,  $k$  is the *step time*,  $x_k^-$  is the predict *state vector*,  $P_k^-$  is the predict *covariance matrix*,  $K_k$  is the *Kalman gain*,  $x_k^+$  is the estimate *state vector*,  $P_k^+$  is the estimate *covariance matrix*,  $A$  and  $H$  are the *Jacobian matrices* of partial derivatives of  $f$  and  $h$  with respect to state variables,  $z$  is the *measurement vector*,  $Q$  is the *process noise covariance matrix* and  $R$  is the *measurement noise covariance matrix*.

## 2.7 Results and analysis

For the estimation of attitude and heading (Euler angles), two procedures were conceived: (a) experimental and (b) computational. In the experimental procedure both the calibration and tests of IMUs were achieved through of a mobile platform in the three axes ( $X$ ,  $Y$  and  $Z$ ), which was manufactured in a 3D printer. The main objective of the platform is to measure the real value of the movement exercised over the IMU. These movements are yielded with a protractor (one for each axis) allowing the user to have a reference of such value. Additionally, the mobile platform facilitates both the calibration and testing procedures. For both IMUs the same equipment was used, which consists mainly of: (a) the platform, (b) an Arduino Nano, (c) a breadboard, (d) the protractors and (e) a ball level (android application). The Figure 6 depicts these platform of IMUs together with the other components.

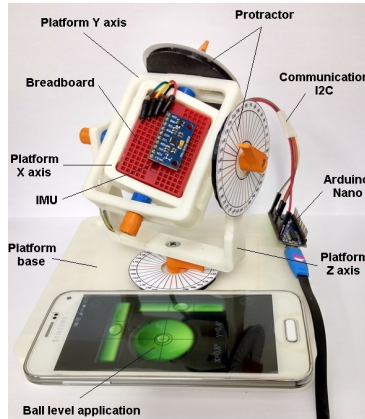


Figure 6. Calibration and tests platform of IMUs

For both calibrations and tests of the IMUs it was taken into account that the mobile platform was well positioned. To achieve that, an Android ball level application was used, in which the 2D tilt can be observed, and thus having control over the position of the platform. Furthermore, the protractors were used to measure the angles at which the IMUs are rotated, these measurements will be used to compare them with regard to the estimates provided by the EKF based sensor fusion technique.

For the calibration procedure the dynamic ranges of  $\pm 250^\circ/sec$ ,  $\pm 2g$  and  $\pm 4800\mu T$  were used for the gyroscope, the accelerometer and the magnetometer, respectively. On the other hand, the calibration was performed by using a different methodology for each sensor. For the gyroscope and accelerometer a static calibration was performed, whereas a dynamic calibration was executed for the magnetometer of the MPU9250. In the case of gyroscope and accelerometer, the IMUs were initially placed on specific positions with the  $Z$  axis perpendicular to the horizontal terrestrial plane and keeping them static. In this calibration process, 100 samples of the 3 axes ( $X$ ,  $Y$  and  $Z$ ) were acquired, from which a maximum and minimum value were obtained in order to determine the *offset value* of the sensors, as stated by Equation 9.

$$offset_{x,y,z} = \frac{max_{x,y,z} + min_{x,y,z}}{2} \quad (9)$$

For the magnetometer the calibration firstly consisted on calibrating the  $X$  and  $Y$  axis and then calibrating the  $Z$  axis, given that the calibration of this sensor must be dynamic for each of the axes, with respect to the same reference magnetic field. This is the reason why the three axes can not be calibrated at the same time. Before performing the calibration, the axis of the magnetometer was adjusted according to Figure 2c. In this case, the sense and direction of the 3 axes ( $X$ ,  $Y$  and  $Z$ ) of this sensor are different with respect to the 3 axes of the gyroscope and accelerometer. For this reason, in the code developed in Arduino the change of assignments of both sense and direction was made so that the 3 sensors have the same configuration with respect to the axes of the gyroscope and accelerometer.

Calibrations for the magnetometer were based firstly on positioning the IMU with the  $Z$  axis perpendicular to the horizontal plane, and then rotating the IMU  $360^\circ$  around this axis, in order to measure the Earth's magnetic field. In this way the  $X$  and  $Y$  axes were calibrated. For calibration of the  $Z$  axis the IMU should be positioned with the  $Y$  axis perpendicular to the horizontal plane, and then rotated the IMU  $360^\circ$  around this axis. The duration of each of the two calibration processes was 20s. The maximum and minimum values were obtained, determining the offset (hard iron part) by using Equation 9 and the scale factor (soft iron part) using Equation 10.

$$scale_{x,y,z} = \frac{max_{x,y,z} - min_{x,y,z}}{2} \quad (10)$$

Figure 7 shows the results before and after calibration procedure of the magnetometer of the MPU9250. In Figure 7a and Figure 7b, the three-dimensional views of both uncalibrated and calibrated measurements are presented respectively, when comparing these figures it can be observed that both have the same shape, but different proportions of both position and length. The measurements in Figure 7a are "useless" data to be applied, since the measurements are not centered on the reference point (0,0,0) of the 3 axes and furthermore, the circumferences have different measurement ratio. In contrast, these two disadvantages are not observed in Figure 7b, since during the calibration process the measurements were positioned and scaled according to the measured magnetic field.

Figure 7c and Figure 7d show the same measurements of the previous case from a 2D perspective. When compared, the difference between uncalibrated and calibrated magnetometer data is better observed. In Figure 7c the measurements of each axis of the magnetometer are very distant from the other axes and completely disproportionate, whereas in Figure 7d the measurements of the 3 axes were correctly calibrated, centralized and scaled.

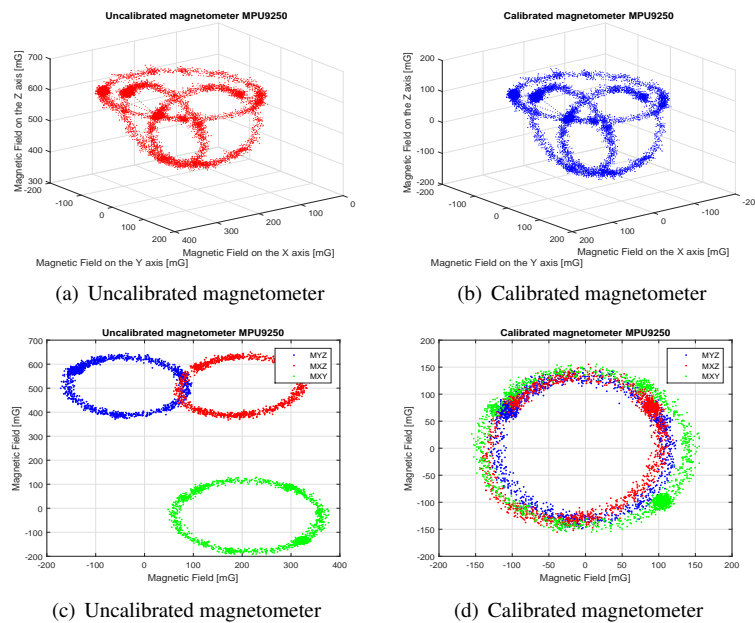


Figure 7. Results of uncalibrated and calibrated magnetometer for MPU6050

The offset and scales values obtained in the previous calibration processes for the 3 sensors, must be taken into account in order to adjust the measurements of each of the sensors. For this, the values of offset and scales must be subtracted from the "raw" measurements of each of the sensors in the Arduino code, where these "raw" values refer to the default measured data provided by each sensor. Therefore, for the output measurements of the gyroscope and for the measurements of the axis  $X$  and  $Y$  of the accelerometer, the output values are given by Equation 11, whereas for the measures corresponding to the axis  $Z$  of the accelerometer the output value is determined by Equation 12. In the case of the magnetometer, Equation 13 represents the model for calculating the output value for the 3 axes of this sensor.

$$Out\ Value = \frac{Raw\ Value - Offset}{Sensitivity\ Scale} \quad (11)$$

$$Out\ Value = 1 + \frac{Raw\ Value - Offset}{Sensitivity\ Scale} \quad (12)$$

$$Out\ Value = \frac{(Raw\ Value - Offset) * Scale}{Sensitivity\ Scale} \quad (13)$$

With regard to the sensor fusion computational procedure two techniques have been used. The first one for *roll* and *pitch* angles and second one for *yaw*. In the case of *roll* and *pitch*, the gyroscope was considered as the system model and the accelerometer as the sensor model in the EKF algorithm. Meanwhile the gyroscope was also used as the system and the magnetometer as sensor for the estimation of the *yaw* angle. For each combination technique, for attitude and heading estimation an EKF was developed and tuned. Figure 8 depicts the configuration of the EKFs sensor fusion modules.

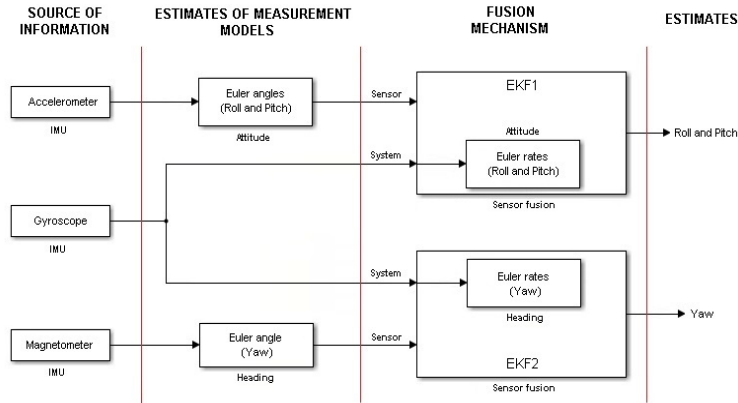


Figure 8. Sensor fusion technique for IMUs

Table 5 presents the parameters selected for the EKF, in order to perform the study of the sensor fusion technique. The selection of these parameters consists of estimating an initial value of the state variables  $x_0$  and the covariance matrix  $P_0$ . The other parameter to configure is the Jacobian matrix  $H$ , which is related to the available sensors for each state variable.

In order to obtain an optimal performance of the EKF, the parameters  $Q$  and  $R$  must be adjusted correctly. To do that, there are two ways of tuning them. The first one is trial and error; that is, to change the values of these covariances until obtaining a good estimate of the state variables. The other method is to adjust  $Q$  according to the reliability of the process model, so that if it is highly reliable a small value can be selected for this parameter. For the  $R$  parameter, a set of sensor measurements must be obtained and then perform a statistical analysis to determine the covariance of the sensor. Another option to determine this parameter is to take a value already used in similar cases for this sensor.

This work took into account that the process model is highly reliable; therefore,  $Q$  is small. Whereas for the sensor ( $R$ ) a value used in a previous work of sensor fusion was taken, to determine the attitude with the linear Kalman filter (KF) (Lauszus, 2015). In EKF1 are two state variables (*roll* and *pitch*) so that the parameters are set in an array of  $2 \times 2$  size, whereas in the case of EKF2, the parameters are scalar because this second fusion mechanism is working with only one state variable (*yaw*).

Table 5. EKF parameters for sensor fusion of the MPU6050 and MPU9250

PARAMETER	Initial values EKF1	Initial values EKF2
$x$	$\begin{bmatrix} 0 \\ 0 \end{bmatrix}$	0
$P$	$\begin{bmatrix} 10 & 0 \\ 0 & 10 \end{bmatrix}$	10
$Q$	$\begin{bmatrix} 0.001 & 0 \\ 0 & 0.001 \end{bmatrix}$	0.001
$R$	$\begin{bmatrix} 0.03 & 0 \\ 0 & 0.03 \end{bmatrix}$	0.03
$H$	$\begin{bmatrix} 1 & 0 \\ 0 & 1 \end{bmatrix}$	1

The tests were achieved through the interaction between the Arduino-Nano and the Matlab R2015 software for reading (the sensors values) and data processing (the filter), respectively. Figure 9 illustrates the results obtained for both *roll* (Figure 9a) and *pitch* angles (Figure 9b) for MPU6050 and Figure 10 shows the results obtained from the estimation of three Euler angles, *roll* (Figure 10a), *pitch* (Figure 10b) and *yaw* (see Figure 10c) for MPU9250. Based on these figures it can be concluded that the noise has been eliminated from the filtered signal (red line) when compared to the accelerometer or magnetometer signal (blue line).

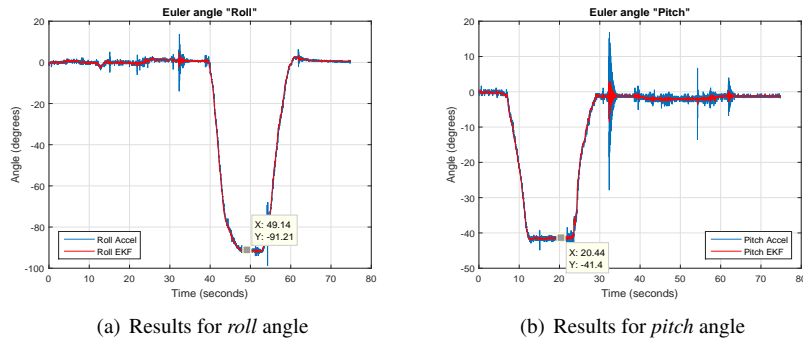


Figure 9. Euler angles estimation for MPU6050

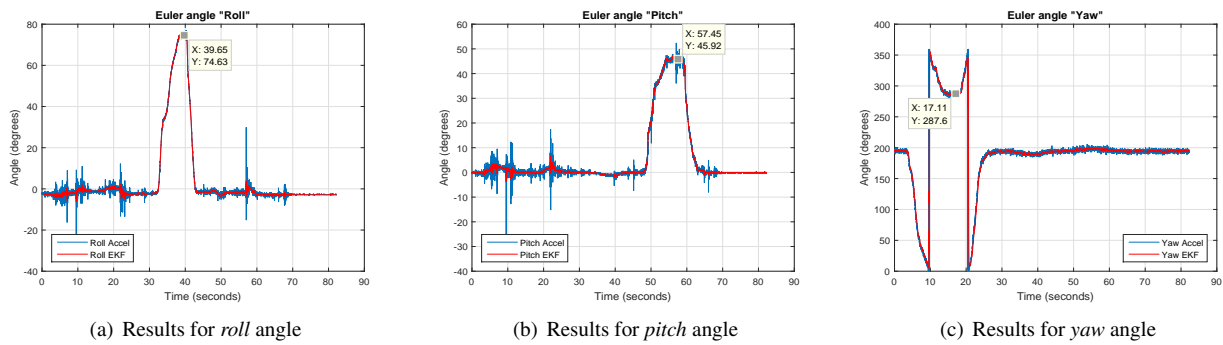


Figure 10. Euler angles estimation for MPU9250

The metric that was used to evaluate the performance of this sensor fusion technique is the Normalized Root Mean Squared Error (NRMSE), which is based on a normalized version of the Root Mean Squared Error (RMSE). Equation 14 presents the model for determining the NRMSE, which is given in units of percentage. Therefore, it can be used for direct comparisons with results from other datasets (with different units of measure) (Spüler *et al.*, 2015).

$$NRMSE = \frac{\sqrt{\frac{\sum_{i=0}^n (\hat{y}_i - y_i)^2}{n}}}{\bar{y}} \quad (14)$$

Table 6 shows the NRMSE results of the Euler angles, for both MPU6050 and MPU9250, which details the good quality of the attitude and heading estimation. The values estimated by the EKFs were compared with the measured values (real) in the calibration and tests platform for IMUs.

Table 6. NRMSE for the MPU6050 and MPU9250

EULER ANGLES	MPU6050	MPU9250
<i>roll</i>	0.0163	0.07
<i>pitch</i>	0.0375	0.0882
<i>yaw</i>	N/A	0.0095

### 3. CONCLUSIONS

In this paper the EKF was used for attitude and heading determination for two IMUs (MPU6050 of 6DOF e MPU9250 of 9DOF) through a sensor fusion technique using two EKF modules, one to estimate *roll* and *pitch* angles, and the other one to estimate *yaw* angle. Two different calibrations were performed, a static calibration for the gyroscope and the accelerometer, and a dynamic calibration for the magnetometer. For the latter sensor two types of calibrations were performed (hard iron and soft iron) with the same sample. Several tests have been made in order to evaluate the performance of this multi-sensor approach. The simulation results obtained have been compared with the real value measurements using a mobile platform designed for calibration and tests of this type of sensors. These platform allows the movement of IMUs in the three axes. The NRMSE performance metric was used to compare the achieved results. The results of NRMSE shows that the EKF based on sensor fusion has good quality for both attitude and heading estimation.

As a proposal of future works taking into account the presented sensor fusion technique (two EKF modules), tests with other IMUs of 9 DOF could be performed, moreover, the UKF or another type of sensor fusion mechanism could be implemented, with the main objective of analyzing and comparing the results of the estimation of *roll*, *pitch* and *yaw* obtained in this work.

#### 4. ACKNOWLEDGEMENTS

This work was supported by FAPDF.

#### 5. REFERENCES

- Ahmad, N., Ghazilla, R.A.R., Khairi, N.M. and Kasi, V., 2013. "Reviews on various inertial measurement unit (imu) sensor applications". *International Journal of Signal Processing Systems*, Vol. 1, No. 2, pp. 256–262.
- Benini, A., Mancini, A. and Longhi, S., 2013. "An imu/uwb/vision-based extended kalman filter for mini-uav localization in indoor environment using 802.15. 4a wireless sensor network". *Journal of Intelligent & Robotic Systems*, pp. 1–16.
- InvenSense, 2011. "Mpu-6000 and mpu-6050 product specification". 25 Sep. 2016.
- InvenSense, 2016. "Mpu-9250 product specification". 8 Mar. 2017.
- Kim, P., 2011. *Kalman filter for beginners: with MATLAB examples*. CreateSpace.
- Kraft, M., 2000. "Micromachined inertial sensors: The state-of-the-art and a look into the future". *Measurement and Control*, Vol. 33, No. 6, pp. 164–168.
- Lauszus, K., 2015. "Kalmanfilter". 13 Apr. 2017 <<https://github.com/TKJElectronics/KalmanFilter/blob/master/Kalman.cpp>>.
- Li, Y. and Xu, X., 2010. "The application of ekf and ukf to the sins/gps integrated navigation systems". In *Information Engineering and Computer Science (ICIECS), 2010 2nd International Conference on*. IEEE, pp. 1–5.
- Ligorio, G. and Sabatini, A.M., 2013. "Extended kalman filter-based methods for pose estimation using visual, inertial and magnetic sensors: Comparative analysis and performance evaluation". *Sensors*, Vol. 13, No. 2, pp. 1919–1941.
- NXP, 2016. "Nxp sensor fusion library for kinetics mcus". *DATA SHEET: PRODUCT PREVIEW, rev*, Vol. 8.
- Ozyagcilar, T., 2015. "Implementing a tilt-compensated ecompass using accelerometer and magnetometer sensors". *Freescale Semiconductor Application Note, rev*, Vol. 3.
- Sacco, M., 2011. "Sensores inerciales: El mundo en movimiento". 1 Aug. 2017 <<http://www.neoteo.com/21690-sensores-inerciales-el-mundo-en-movimiento>>.
- Spüler, M., Sarasola-Sanz, A., Birbaumer, N., Rosenstiel, W. and Ramos-Murguialday, A., 2015. "Comparing metrics to evaluate performance of regression methods for decoding of neural signals". In *Engineering in Medicine and Biology Society (EMBC), 2015 37th Annual International Conference of the IEEE*. IEEE, pp. 1083–1086.
- Winer, K., 2015. "Simple and effective magnetometer calibration". 22 Mai. 2017 <<https://github.com/kriswiner/MPU6050/wiki/Simple-and-Effective-Magnetometer-Calibration>>.
- Zhao, H. and Wang, Z., 2012. "Motion measurement using inertial sensors, ultrasonic sensors, and magnetometers with extended kalman filter for data fusion". *IEEE Sensors Journal*, Vol. 12, No. 5, pp. 943–953.

#### 6. RESPONSIBILITY NOTICE

The following text, properly adapted to the number of authors, must be included in the last section of the paper:  
The author(s) is (are) the only responsible for the printed material included in this paper.